Made-to-Measure Outperforms Schwarzschild's Method

Richard J. Long

Department of Astronomy, Westlake University, Hangzhou, Zhejiang 310030, China;

rjlastro@yahoo.com; Orcid:0000-0002-8559-0067

Abstract Syer and Tremaine's made-to-measure method and Schwarzschild's orbit superposition method are well-known within the field of stellar dynamical modeling. This research is concerned with assessing and comparing the operational capabilities of the two methods and, in particular, the impact on observable reproduction, orbit classifications and computer elapsed times when using low orbit numbers (8000 orbits) with different observational data sets and initial conditions. Both methods are able to reproduce observed data with mean $\chi^2 \approx 1$ or less. However, the made-to-measure process does so three to five times faster than the orbit superposition method, and this starts to make the made-to-measure process attractive for analysing galaxy surveys. For a given set of initial conditions, both methods produce similar orbit classifications but the orbits behind the classifications are not the same. Orbits which are common do not have the same weights. Different initial conditions result in

Key words: galaxies: kinematics and dynamics – galaxies: structure – methods: numerical

1 INTRODUCTION

different classifications.

Syer and Tremaine's made-to-measure method (Syer & Tremaine, 1996) (M2M) and Schwarzschild's orbit superposition method (Schwarzschild, 1979) (SCHW) are well-known within the field of stellar dynamical modeling. Of the two, SCHW has more citations (885) at the time of preparing this article (mid-2025) than M2M (168). M2M and SCHW have been compared previously in Long & Mao (2012) where M2M and SCHW were shown to be able to produce similar estimates of galaxy mass-to-light ratios. It is now appropriate that a further comparison is made.

Three factors are relevant.

- 1. Data sizes have increased both in terms of the numbers of galaxies being surveyed and the numbers of spaxels being used to capture galaxy data, and will continue to increase. Internally, because of its orbit weighting mechanism, SCHW is not well structured to deal with the increases expected. M2M is much better positioned.
- 2. Galaxy surveys would benefit from being analyzed by methods such as M2M and SCHW with their abilities to handle data from multiple surveys, data of different types (spaxel and discrete), chemical

Table 1: Abbreviations

Abbreviation	Meaning
3I	three integral initial conditions
$ATLAS^{3D}$	relating to the ATLAS ^{3D} survey
GPU	graphics processing unit
hmdtu	half mass dynamical time unit (galaxy specific time unit)
IFU	integral field unit
M2M	relating to the made-to-measure method
MDJV	'match density Jeans velocities' initial conditions
MGE	multi-Gaussian expansion
MPI	message passing interface
M/L	mass-to-light
NNLS	non-negative least squares
PC	personal computer
SCHW	relating to Schwarzschild's method

data, population synthesis data and orbit classification constraints. However both M2M and SCHW appear to be too slow to handle survey scale activities.

3. An improved understanding of what methods such as M2M and SCHW are capable of doing, or not doing. For example, M2M and SCHW can only weight the orbits that have been provided to reproduce the observed data. At best, the models produced may only be illustrative of what the real galaxy might be like. At worst, the models are non-physical.

This article will not address the third factor: this may be better left to machine learning. The first two factors will be considered further. At the time of the first comparison, the accepted assessment was that M2M, with its ability to use significantly more orbits (numbers of 10^5 to 10^6 were not uncommon), must of course be producing the better models. SCHW by comparison was claimed to model real galaxies with only a few hundred orbits. The question being posed in this article is how does M2M compare with SCHW when run using fewer orbits, for example $\approx 10^4$. The objective of this research therefore is to assess and compare the operational capabilities of M2M and SCHW, in particular the impact on observable reproduction, orbit classifications and computer elapsed times, when using low orbit numbers.

The article's structure is as follows. Section 2 summarizes at a top level the approach taken in the investigation. The observational data are described in Section 3, with methods and techniques in Section 4. Results and subsequent discussion are in Sections 5 and 6, with conclusions in Section 7. The main abbreviations used are defined in Table 1.

2 APPROACH

The Introduction, Section 1, sets the context and describes *what* is to be investigated. This Approach section describes *how* the investigation is performed. In this case, the approach is straightforward: it is just a simple combinatorial problem of running a number of models using different methods, initial conditions, and data sets. The results required for comparison purposes are

• the observable mean χ^2 values indicating how well the model has reproduced its observational data,

- the computer elapsed time for the modeling runs, and
- the orbit classifications giving the weighted hot, warm, cold and counter-rotating orbit fractions supporting reproduction of the observables.

The assessment of the performance of M2M relative to SCHW will be based on these comparisons. Gravitational potentials and initial conditions are specific to the observational data, and are only calculated once since they will be reused whenever the observational data are used. Data layouts (for example, using a polar grid or Voronoi cells) are not changed except for one set of very specific tests. For other parameters, such as the duration of model runs, their values are kept the same for both the M2M and SCHW runs.

In outline, there are

- two methods, M2M and SCHW;
- two sets of initial conditions, theoretically based (3I) and observationally based (MDJV); and,
- two top level data sets, real galaxy data (ATLAS^{3D}) and simulated galaxy data (IllustrisTNG).

More information is provided in Sections 3 and 4.

It is not intended that the behavior and performance of all the capabilities of M2M will be compared with all the capabilities of SCHW but only the core capabilities concerned with luminosity and kinematical data reproduction. Features such as discrete data handling, or chemical modeling, or orbit classification constraints are out of scope, as is parameter estimation using the methods. Note also that only axisymmetric (oblate) models are utilized: the investigations are not affected by choice of gravitational potential. The kinematical observables are varied so that both velocity moments and Gauss-Hermite coefficients are modeled - see Section 3. The earlier comparison in Long & Mao (2012) used Gauss-Hermite coefficients only.

SCHW requires the use of NNLS software to create orbit weights, We choose NNLS software that implements the Lawson and Hanson active set method (Lawson & Hanson, 1974) since it appears from the literature to be the most used NNLS implementation for SCHW. The active set algorithm deliberately zeroises the weights of any orbits it chooses not to use in reproducing the observed data, and this is taken into account in the analysis software used.

Model selection frameworks such as Lipka & Thomas (2021) and Thomas & Lipka (2022) are not used. Some use is made of an experimental Gaussian processes approach to M2M hyper-parameter determination.

Other than to compare M2M and SCHW orbit classifications for IllustrisTNG data with Xu et al. (2019), no external comparisons of models are made.

3 OBSERVATIONAL DATA

The observational data sets used in this article are the same as those used in Long (2025). The data tables here are modified versions of the tables from that paper.

For the ATLAS^{3D} data set (Cappellari et al., 2011), data from four galaxies are utilized - NGC 1248, NGC 3838, NGC 4452, and NGC 4551. These galaxies have various inclinations, different mass-to-light ratios, and sense of bulk rotation (see Table 2). Surface brightness values are calculated using multi-Gaussian

Table 2:	Top level	data for the	$ATLAS^{3D}$	galaxies
----------	-----------	--------------	--------------	----------

Galaxy	Inclination	M/L ratio	Type	Bulk rotation	SB max radius	IFU cells
NGC 1248	42°	2.50	S0	Counter clockwise	3.00	297
NGC 3838	79°	4.00	S 0	Clockwise	5.86	383
NGC 4452	88°	5.20	S0	Clockwise	5.17	489
NGC 4551	63°	4.89	E	Counter clockwise	3.41	596

The inclinations are taken from Cappellari et al. (2013), while the M/L ratios were determined by M2M modeling in Long (2016). The SB max radius column gives the overall size of the polar grid used for surface brightness data values. The IFU column gives the number of Voronoi cells for the kinematical data.

Table 3: Top level data for the simulated galaxies

Galaxy	Bulk rotation	SB max radius	IFU cells
A0490	Counter clockwise	7.00	220
A1090	Counter clockwise	6.00	197
A1190	Clockwise	6.00	110
A1290	Clockwise	6.00	173
A1390	Clockwise	7.00	119

As in Table 2, the SB max radius column gives the overall size of the surface brightness polar grid, and the IFU column gives the number of Voronoi cells. Inclinations for all the simulated galaxies are 90° , and mass-to-light ratios are 1.0.

expansions (Sect. 4.1). The IFU cells for kinematical data (first and second velocity moments) are the Voronoi cells resulting from signal-to-noise processing of the raw data.

For the IllustrisTNG galaxies (Nelson et al., 2019), five axisymmetric galaxies (A0490, A1090, A1190, A1290, and A1390) are utilized, and are viewed edge on with the mass-to-light ratio taken as 1.0 for all galaxies. Surface brightness values are again calculated using multi-Gaussian expansions. The IFU cells for kinematical data (the Gauss-Hermite coefficients h_1 to h_4) are constructed to represent a real galaxy's data (see Table 3).

For both data sets, data values are symmetrized appropriately for an axisymmetric model/potential. The units used are effective radii for length, 10^7 years for time, and mass in units of the solar mass with luminosity similarly so.

4 METHODS

With the exception of M2M, all the methods and techniques in this section are very similar to those in Long (2025) and are not described in detail here. The M2M implementation was used recently in Long et al. (2021), and is described more fully in Long (2016) and other papers by the lead author prior to that.

4.1 Gravitational Potentials

The gravitational potentials and their derivatives used for modeling are derived from MGEs of the surface brightness data (Emsellem et al., 1994; Cappellari, 2002). For the IllustrisTNG simulated data, dark matter potentials are included as spherical Gaussians, and no black hole modeling takes place. For the ATLAS^{3D} data, no dark matter is included for consistency with Cappellari et al. (2013), and central black holes are modeled as point sources.

4.2 Orbit Initial Conditions

Initial phase space coordinates for stellar orbits are created using the 3I scheme (theoretically based) and the MDJV scheme (observationally based). These initial coordinates are given an overall sense of rotation matching that shown by the observed mean line-of-sight velocity data, with 75% of the orbits having the same sense of rotation and 25% counter-rotating. In general, 8000 orbits are used for most of the modeling of the observed data sets. For ATLAS^{3D} galaxies NGC 3838 and NGC 4452, 16000 orbits are used instead so that the elapsed time impact on the SCHW NNLS process, in particular, may be assessed.

4.3 Orbit Classifications

The circularity measure λ_z (Zhu et al., 2018) is used to classify orbits into one of hot ($|\lambda_z| <= 0.25$), cold ($\lambda_z >= 0.80$), warm (0.25 < $\lambda_z < 0.8$) or counter-rotating. The total orbit weights in each of the classes are taken as the overall orbit classification for a galaxy. Comparing orbit classifications produced by M2M and SCHW is a key part of our modeling analysis. Note that orbit classifications are not used as constraints themselves, as in Long (2025). However, the sum of the weights is constrained to be equal to one, and so the sum of the orbit classes must also equal one.

4.4 SCHW Models

SCHW has three main phases in its execution.

Phase 1 Using the initial conditions as orbit start coordinates, orbit trajectories are created in the gravitational potential that has been associated with the observed data. The phase space coordinates representing the trajectories are used to construct the individual orbits' contributions to the model equivalents of the observed data. Phase 1 completes once a predetermined number of orbit integration time steps or orbits have been completed.

Phase 2 The individual orbit contributions are weighted in a non-negative least squares sense (NNLS) such that the model observables reproduce as closely as possible the observed data. Any regularization constraints are included in this phase.

Phase 3 The weighted orbits are analyzed as necessary to learn more about the observed data.

For use with SCHW, the observed data must be modified so that it is surface luminosity (or mass) weighted. In addition, for this investigation, regularization is used (heavy weights penalization) in order to make realistic comparisons with M2M possible (see Sections 4.5 and 5.1).

No use of SCHW dithering (orbit bundling) is made as it causes a significant performance overhead for SCHW.

4.5 M2M Models

M2M differs from SCHW in that *phase 1* and *phase 2* are combined into a single phase in which the weights exist from the start of modeling and are iteratively adapted, as the orbit trajectories are traversed, such that the model observables (calculated using the weights) eventually reproduce the observed data. This iterative adaption of the weights is akin to the back-propagation mechanism in machine learning neural networks.

M2M terminates in a similar fashion to SCHW phase 1. On termination, an extra condition must be met which is that the weights should have converged to constant values (to within some numerical tolerance).

Exponential smoothing is used by default in the construction of M2M model observables. This smoothing mechanism could be turned off but, for the low number of orbits used here, results in much noise within the model, for example in the observable χ^2 series. The preferred approach here is to regularize SCHW instead (see Sections 4.5 and 5.1) to achieve an approximate balance in behavior of the two methods.

4.6 Hyper-parameters using Gaussian Processes

Both modeling methods require a number of hyper-parameters to be set, for example, the ϵ learning rate parameter in M2M, or the regularization parameter in SCHW. In general, these parameters have been set by a combination of experience and experimentation. During this investigation, an experimental routine using Gaussian processes was developed using the *scikit-optimize* package's *gp_minimize* interface. This routine was used to good effect to confirm some of the M2M ϵ settings, and also to demonstrate that M2M can be used successfully inside a more general framework application.

4.7 Software Utilization

As in Long (2025), the software base for constructing initial conditions and for M2M and SCHW modeling is the lead author's implementation of the Syer & Tremaine (1996) M2M stellar dynamical modeling method together with the Schwarzschild (1979) orbit superposition method (a single code set supports both methods). This software was first used in Long & Mao (2010), and, as indicated, more recently in Long (2025). The software is Python 3 based with some use of Cython (Behnel et al., 2011) and C for performance critical code. The MPI message passing interface is used to achieve parallelization of orbit integration, with the same number of cores being used for both M2M and SCHW. The optimization software used for NNLS is taken from the SCIPY package version 1.16 (Virtanen et al., 2020) (earlier versions may have NNLS performance issues). The Gaussian processes application is based on routines within the publicly available *scikit-optimize* package. Using a 20 core desktop PC, multi-processor working is employed with up to 10 cores active in a modeling run.

5 RESULTS

Most of the column headings in the tables within this section should be self-explanatory. However, for clarity,

- 'Active orbits' refers to the number of orbits that have a non-zero weight while 'Orbits' indicates the number of orbits in the initial conditions.
- Under 'Mean χ^2 values', 'sb los v1 los v2' indicates surface brightness and the line-of-sight first and second velocity moments. 'sb h_1 h_2 h_3 h_4 ' indicates surface brightness and the Gauss-Hermite coefficients h_1 to h_4 .
- Under 'Orbit classification', 'Hot Warm Cold C-R' refers to the hot, warm, cold and counter-rotating class values described in Section 4.3.

As an aid to the reader, tables used in comparing orbit classification results employ colored text to indicate differences of $\geq 3\%$ (as in Long 2025). What is important in these tables is to be clear on the direction the comparison is being made (horizontally or vertically between sections in the tables), and to use the colors to gain a visual impression of the extent of any disagreement. For example, a table section with few colored entries means few differences implying results are similar; conversely, many colored entries imply that results are dissimilar. Note that the sum of the orbit classes in a classification for a galaxy, as stated in Section 4.3, must be one. This means that an increase or decrease in one class value must result in decreases or increases in one or more other class values.

5.1 Regularizing SCHW

In order to ensure a more balanced comparison between M2M and SCHW, a regularized form of SCHW is used in which heavy weights are penalized. This has a comparable end effect to the exponential smoothing used in M2M, and helps to ensure that the orbit weights of SCHW and M2M in integral space are smoothed to a similar degree. This is illustrated in Figure 1 using models created with the ATLAS^{3D} data for NGC 4452. The other ATLAS^{3D} galaxies and the IllustrisTNG galaxies behave similarly. Smoothness in Figure 1 is calculated as the second derivative of the weights with respect to energy, and to the z-component of angular momentum. As may be seen from the figure, the unpenalized SCHW plots are considerably less smooth than the penalized versions, with penalized SCHW exhibiting a similar degree of smoothness to M2M. In addition, the impact of heavy weights penalization is to bring the SCHW weight range closer to that of M2M, and also to increase the number of active orbits in SCHW. For NGC 4452, the M2M weight range is $(7.09 \times 10^{-7}, 1.71 \times 10^{-3})$ and the number of active orbits is 15963. For SCHW, the range is $(2.35 \times 10^{-6}, 5.02 \times 10^{-2})$ with 635 active orbits without penalization, and $(3.03 \times 10^{-9}, 1.01 \times 10^{-3})$ and 13106 active orbits with penalization. These points provide the background to our choice of penalized SCHW for M2M versus SCHW comparisons.

5.2 χ^2 and Elapsed Time Comparisons between M2M and SCHW

The focus in this section is on how well observed data are reproduced, and comparing modeling elapsed times. Orbit classifications are considered in the next section. M2M and SCHW models using both 3I and MDJV initial conditions and both data sets are created. Table 4 contains the results for the ATLAS^{3D} galaxy data, and Table 5 for the IllustrisTNG galaxy data. In the tables, all the mean observable χ^2 values are ≈ 1 or less indicating that the observed data have been well-reproduced by both M2M and SCHW. An example is shown in Appendix A. M2M weight convergence values are > 93% implying that convergence to constant weights, as expected in Syer & Tremaine (1996), is close to being achieved. For ATLAS^{3D}, the modeling elapsed times show that M2M performs faster than SCHW by a factor of ≈ 4 for 8000 orbit models and by ≈ 5 for 16000 orbit models. For IllustrisTNG data, M2M outperforms SCHW by a factor of ≈ 3 . Any of these performance improvement factors would benefit large surveys where there are thousands of galaxy data sets to be processed. The NNLS contributions to SCHW elapsed times show that, with increasing model size (numbers of orbits in this case), the performance difference will become more marked depending on the algorithms within the NNLS implementation.

SCHW with no penalization SCHW penalized M2M E - weight E - weight 0.75 0.75 0.75 0.50 0.50 0.50 Smoothness Smoothness 0.25 0.25 Smoothness 0.25 0.00 0.00 0.00 -0.25 -0.25 -0.25 -0.50 -0.50 -0.50 -0.75 -0.75 -0.75 weight L2 - weight Lz - weight 1.00 1.00 1.00 0.75 0.75 0.75 0.50 0.50 0.50 Smoothness Smoothness 0.25 0.25 0.25 0.00 0.00 0.00 -0.25 -0.25 -0.25 -0.50 -0.75 -0.75 -1.00 -1.00 -1.00

Fig. 1: Heavy Weights Penalization illustrated with NGC 4452

Heavy weights penalization illustrated with NGC 4452 (Section 5.1). Smoothness is calculated as the second derivative of the weights with respect to the two integrals (E and L_z). As may be seen from the figure, the unpenalized SCHW plots show considerably more variation than penalized SCHW. Penalized SCHW, using a parameter value of 1.6×10^3 , shows a similar degree of smoothness to M2M.

5.3 Orbit Classification Comparisons between M2M and SCHW

The comparisons between orbit classification results from modeling with M2M and SCHW are shown in Table 6. M2M and SCHW are producing similar orbit classifications from the same observed data and initial conditions, with ATLAS^{3D} and MDJV showing the most variation in classification and IllustrisTNG and MDJV showing the least.

Orbit classifications are compiled from individual orbits and, given that here the same sets of orbits (initial conditions) are used for M2M and SCHW modeling, whether or not M2M and SCHW are using the same orbits in the same classifications is investigated. Table 7 shows how many orbits are common to both modeling methods, and how many are specific to one of M2M or SCHW. Comparatively few are specific to SCHW only, with substantially more being specific to M2M. This is readily explainable: orbits which are zero weighted by SCHW appear in the M2M only figures.

The next step is to look in detail at the common orbits, to investigate whether individual orbits are weighted similarly by M2M and SCHW. Figure 2 contains various plots from considering just the ATLAS 3D data set modeled with 3I initial conditions. The left hand scatter plots show the paired orbit weights arising from M2M and SCHW modeling, with the **blue** dashed line indicating equality of the orbit weights. The key point to note is that the weights are not tightly positioned close to the equality line: even though the orbits used are the same, M2M and SCHW are in general not allocating the same weights to the orbits. The central Bland-Altman plots of the average log weight for an orbit against the log difference between its M2M weight and its SCHW weight show that the mean log difference (**red** solid line) is approximately zero (absolute values $< 10^{-2}$) indicating that there is no significant bias towards either method. In ad-

Table 4: ATLAS $^{\mathrm{3D}}$ M2M and SCHW 3I and MDJV Comparisons - $\chi 2$ and Elapsed Times

		Model	M	ean χ^2 va	lues	M2M Weight	Elapsed	
Galaxy	Orbits	Duration	sb	los v1	los v2	Convergence	Time	
		(hmdtu)					(s)	
3I- M2M								
NGC 1248	8000	200	0.31	0.27	0.63	99%	358	
NGC 3838	16000	500	1.07	0.18	0.57	96%	1065	
NGC 4452	16000	200	0.76	0.42	0.69	96%	865	
NGC 4551	8000	200	0.41	0.19	0.76	100%	217	
3I- SCHW								
NGC 1248	8000	200	0.07	0.11	0.28		1407	(228)
NGC 3838	16000	500	0.19	0.09	0.18		5024	(1379)
NGC 4452	16000	200	0.30	0.13	0.25		4555	(1524)
NGC 4551	8000	200	0.06	0.07	0.23		900	(238)
MDJV - M2M								
NGC 1248	8000	200	1.06	0.11	0.30	96%	561	
NGC 3838	16000	500	0.91	0.35	0.33	93%	1229	
NGC 4452	16000	200	1.08	0.52	1.12	94%	1008	
NGC 4551	8000	200	0.52	0.16	1.33	98%	252	
MDJV - SCHW								
NGC 1248	8000	200	0.05	0.12	0.36		1486	(225)
NGC 3838	16000	500	0.12	0.13	0.21		5422	(1392)
NGC 4452	16000	200	0.56	0.23	0.44		4763	(1422)
NGC 4551	8000	200	0.10	0.07	0.32		1012	(267)

 $\chi 2$ and elapsed time M2M and SCHW comparison using ATLAS 3D data (Section 5.2). All the mean observable χ^2 values are ≈ 1 or less indicating that the observed data have been well-reproduced by both M2M and SCHW. The M2M weight convergence is > 90%. The SCHW χ^2 values are less than those for M2M due to over-fitting of the observed data (as expected). M2M performs faster than SCHW in elapsed times by a factor of ≈ 4 for 8000 orbit models and by ≈ 5 for 16000 orbit models. The numbers in brackets are the NNLS contributions to the elapsed times. With increasing numbers of orbits, the performance difference will become more marked depending on the NNLS implementation used by SCHW.

dition, weight differences are larger at lower average weights than with higher average weights. The red dashed lines show the 2.5% and 97.5% percentiles with 95% of the difference ratios lying between the lines. Expressing the values of the percentiles as percentages, they are equivalent to saying that the weight differences range from a few tens of percent lower to a few hundred percent higher. The right hand plots show the distributions of the weight ratios. The red lines have the same meaning as in the Bland-Altman plots.

Finally, it is useful to note that if in a model orbit weights are sorted into descending order, then just how many orbits contribute to the heaviest 25%, 50%, 75% and 100% by weight can be established. Using 3I initial conditions, the approximate profile for ATLAS^{3D} is [8%, 22%, 44%, 100%] of the orbits, and for IllustrisTNG [4%, 14%, 35%, 100%]. What is then clear is the first 25% of the total weight involves a small number of heavily weighted orbits, while over 50% orbits (lightly weighted) make up the final 25%. Both M2M and SCHW are affected in the same way.

Table 5: IllustrisTNG M2M and SCHW 3I and MDJV Comparisons - $\chi 2$ and Elapsed Times

		Model		Mea	$n \chi^2 va$	lues		M2M Weight	Elapsed	
Galaxy	Orbits	Duration	sb	h_1	h_2	h_3	h_4	Convergence	Time	
		(hmdtu)							(s)	
3I - M2M										
A0490	8000	200	0.94	0.72	1.10	0.66	1.23	96%	1203	
A1090	8000	100	0.87	0.93	1.04	0.63	0.61	93%	632	
A1190	8000	100	0.75	0.79	0.92	0.84	0.56	97%	738	
A1290	8000	100	0.71	1.01	0.94	0.77	0.73	93%	550	
A1390	8000	100	0.90	0.85	1.24	0.61	0.56	96%	628	
3I - SCHW										
A0490	8000	200	1.30	0.39	0.72	0.43	0.89		3746	(196)
A1090	8000	100	0.54	0.49	0.59	0.25	0.31		1948	(200)
A1190	8000	100	0.53	0.35	0.73	0.20	0.39		2240	(197)
A1290	8000	100	0.33	0.37	0.41	0.23	0.38		1816	(200)
A1390	8000	100	0.69	0.42	0.88	0.28	0.35		2037	(200)
MDJV - M2M										
A0490	8000	100	1.04	0.75	0.79	0.54	1.07	96%	753	
A1090	8000	100	0.78	0.88	1.01	0.52	0.43	95%	776	
A1190	8000	100	0.61	0.60	0.58	0.43	0.53	96%	858	
A1290	8000	100	1.21	0.70	0.68	0.64	0.54	97%	665	
A1390	8000	100	0.85	0.81	1.06	0.46	0.44	96%	776	
MDJV - SCHW										
A0490	8000	100	0.43	0.20	0.21	0.21	0.42		1939	(235)
A1090	8000	100	0.54	0.31	0.42	0.24	0.20		2180	(257)
A1190	8000	100	0.26	0.22	0.31	0.15	0.21		2336	(267)
A1290	8000	100	0.37	0.29	0.24	0.15	0.21		1865	(258)
A1390	8000	100	0.48	0.33	0.44	0.20	0.25		2193	(258)

 $\chi 2$ and elapsed time M2M and SCHW comparison using IllustrisTNG data (Section 5.2). All the observable χ^2 values are ≈ 1 or less indicating that the observed data have been well-reproduced by both M2M and SCHW with, for M2M, the weight convergence being > 90%. M2M outperforms SCHW by a factor of ≈ 3 in elapsed times. As in Table 4, the numbers in brackets are the NNLS contributions to the elapsed times.

5.4 Comparisons between 3I and MDJV

The orbit classification results achieved with 3I and MDJV initial conditions are compared for M2M and SCHW using both 3I and MDJV initial conditions. The comparisons are shown in Table 8. The numerical values in Table 8 are the same as Table 6 but this time the comparisons are made horizontally (3I versus MDJV) rather than vertically (M2M versus SCHW). From the coloring used, it should be apparent from Table 8 that 3I and MDJV initial conditions do not produce the same orbit classifications. The only class where there is some agreement is with the counter-rotating orbits.

5.5 Comparison with Xu et al. (2019)

The orbit classification comparisons for M2M and SCHW using IllustrisTNG data in Section 5.3 are compared with Xu et al. (2019), and the results recorded in Table 9. Apart from the A0490 M2M model, all the other models have differences with Xu et al. (2019) in the hot, warm and cold classifications and this

Table 6: M2M versus SCHW Comparisons for 3I and MDJV - Orbit Classifications

		3I Init	ial Condi	tions		l	MDJV I	nitial Con	ditions	
Galaxy	Active	(Orbit Clas	sificatio	n	Active	(Orbit Clas	sificatio	n
	Orbits	Hot	Warm	Cold	C-R	Orbits	Hot	Warm	Cold	C-R
Atlas3D – M2M										
NGC 1248	7977	0.18	0.41	0.23	0.17	8000	0.24	0.43	0.21	0.12
NGC 3838	14098	0.16	0.37	0.36	0.11	13742	0.27	0.51	0.16	0.06
NGC 4452	15896	0.17	0.31	0.34	0.17	15389	0.25	0.49	0.12	0.14
NGC 4551	7889	0.26	0.39	0.15	0.19	7882	0.39	0.46	0.03	0.13
Atlas3D – SCHW										
NGC 1248	7878	0.19	0.42	0.25	0.13	7804	0.25	0.45	0.17	0.13
NGC 3838	10484	0.22	0.39	0.31	0.07	12440	0.23	0.56	0.15	0.07
NGC 4452	13106	0.19	0.31	0.31	0.18	8678	0.19	0.51	0.13	0.17
NGC 4551	7771	0.30	0.38	0.13	0.18	7225	0.33	0.48	0.03	0.16
IllustrisTNG – M2M										
A0490	8000	0.36	0.28	0.13	0.23	8000	0.36	0.34	0.09	0.21
A1090	8000	0.30	0.43	0.15	0.12	8000	0.34	0.46	0.09	0.11
A1190	8000	0.39	0.40	0.08	0.13	8000	0.42	0.41	0.04	0.13
A1290	8000	0.31	0.34	0.20	0.14	7977	0.34	0.37	0.15	0.14
A1390	8000	0.33	0.42	0.12	0.13	8000	0.34	0.46	0.06	0.13
IllustrisTNG - SCHW										
A0490	4529	0.38	0.31	0.14	0.18	6084	0.37	0.34	0.09	0.20
A1090	5315	0.30	0.41	0.18	0.11	6906	0.35	0.46	0.10	0.10
A1190	5581	0.40	0.37	0.10	0.13	7379	0.43	0.40	0.04	0.13
A1290	5135	0.30	0.36	0.21	0.13	6984	0.34	0.38	0.15	0.13
A1390	5739	0.33	0.40	0.13	0.13	7219	0.35	0.46	0.06	0.12

Orbit classification comparisons for M2M and SCHW with both 3I and MDJV initial conditions (see Section 5.3). Comparisons in the table are made vertically, first between M2M and SCHW using ATLAS $^{\rm 3D}$ data, and then using IllustrisTNG data. Classification differences of $\geq 3\%$ between M2M and SCHW are indicated in **blue**. M2M and SCHW are producing similar orbit classifications from the same observed data, with ATLAS $^{\rm 3D}$ and MDJV showing the most variation (top right 'partition') and IllustrisTNG and MDJV showing the least (bottom right 'partition'). The largest individual variation is 6% and occurs in the hot classifications for ATLAS $^{\rm 3D}$ data.

is considered further in the Discussion (Section 6). Apart from the counter-rotating classification for the A0490 SCHW model, all other counter-rotating classifications agree, to within 3%, with Xu et al. (2019). The differences in the MDJV cold column reflect the fact that MDJV produces fewer cold orbits than 3I, and does not meet the orbital needs of the observed data.

5.6 Impacts of Changing Data Layout

In this section, the impact of interpolating the IFU kinematical data from their Voronoi cells onto a polar grid is considered. The polar grid chosen has 8 divisions logarithmically in radius and 32 in angle (making up 2π radians). The Voronoi observed data are interpolated onto this (8,32) polar grid using 'nearest point' interpolation (see Figure 3). The modeling runs are limited to M2M with 3I initial conditions and ATLAS^{3D} galaxy data only: no use is made of SCHW, MDJV or IllustrisTNG data for this part of the investigation.

Table 7: M2M versus SCHW Orbit Comparison

		3I Iı	nitial Conditi	ons			MDJV	Initial Cond	litions	
Galaxy	Active	e Orbits	Common	M2M	SCHW	Active	e Orbits	Common	M2M	SCHW
	M2M	SCHW	Orbits	only	only	M2M	SCHW	Orbits	only	only
$\mathbf{ATLAS}^{\mathrm{3D}}$										
NGC 1248	7992	7886	7843	149	3	7985	7812	7759	226	9
NGC 3838	15947	10528	10087	4992	290	15763	12475	12241	2645	113
NGC 4452	15963	13106	12910	3053	20	15992	8678	8587	7251	7
NGC 4551	7975	7780	7726	232	22	7955	7225	7158	797	7
IllustrisTNG										
A0490	7993	4563	4519	3474	0	8000	6087	6032	1968	0
A1090	8000	5315	5259	2741	0	8000	6906	6855	1145	0
A1190	8000	5581	5523	2416	0	8000	7390	7339	661	0
A1290	8000	5135	5074	2926	0	8000	6992	6926	1045	11
A1390	8000	5739	5684	2316	0	8000	7219	7165	823	0

M2M versus SCHW orbit comparisons (Section 5.3) using both sets of initial conditions and both data sets. The comparison for every galaxy's data shows the number of orbits which are common to both M2M and SCHW models, and those that are particular to just one model. Zero-weighted orbits in SCHW models, if they are used by M2M, are accounted for in the M2M only subset. This explains the comparatively small values in the SCHW only column, and the much larger values in the M2M only column. The common orbits are examined in more detail in Figure 2.

No issues with observable χ^2 values were noted and the M2M weights converged as required (Table 10). Orbit classification values are in Table 11. Nine differences $\geq 3\%$ are recorded, with the maximum difference being 9%. Overall, it appears that the geometric arrangement of the observed data does influence the orbit classifications obtained. Given the results obtained in the investigation as a whole, it is considered unlikely that the geometric effect is M2M specific and does not affect SCHW as well.

The impact of changing the surface brightness layout is now briefly considered. Taking one galaxy's ATLAS $^{\rm 3D}$ data (NGC 4551), 3I initial conditions, and modeling with M2M, the following polar grid layouts are employed: (16,8) and (8,16) with uniform radial intervals, and (16,16) with uniform and logarithmic radial intervals. This gives four different surface brightness layouts. The kinematical data are unmodified from the IFU data used for the NGC 4551 3I modeling run in Table 4. The results obtained for the four modeling runs are

- 1. the mean χ^2 values for surface brightness range from 0.14 to 0.41,
- 2. the χ^2 values for the first and second velocity moments are the same for all runs,
- 3. M2M weight convergence is > 99%, and
- 4. the orbit classifications are the same for all runs to within 1%.

In short, varying the surface brightness polar layout in isolation has had little effect on the modeling results achieved. This clearly differs from the kinematical data results described above.

6 DISCUSSION

The Results (Section 5) contain many tables and much detail so the main findings are summarized below.

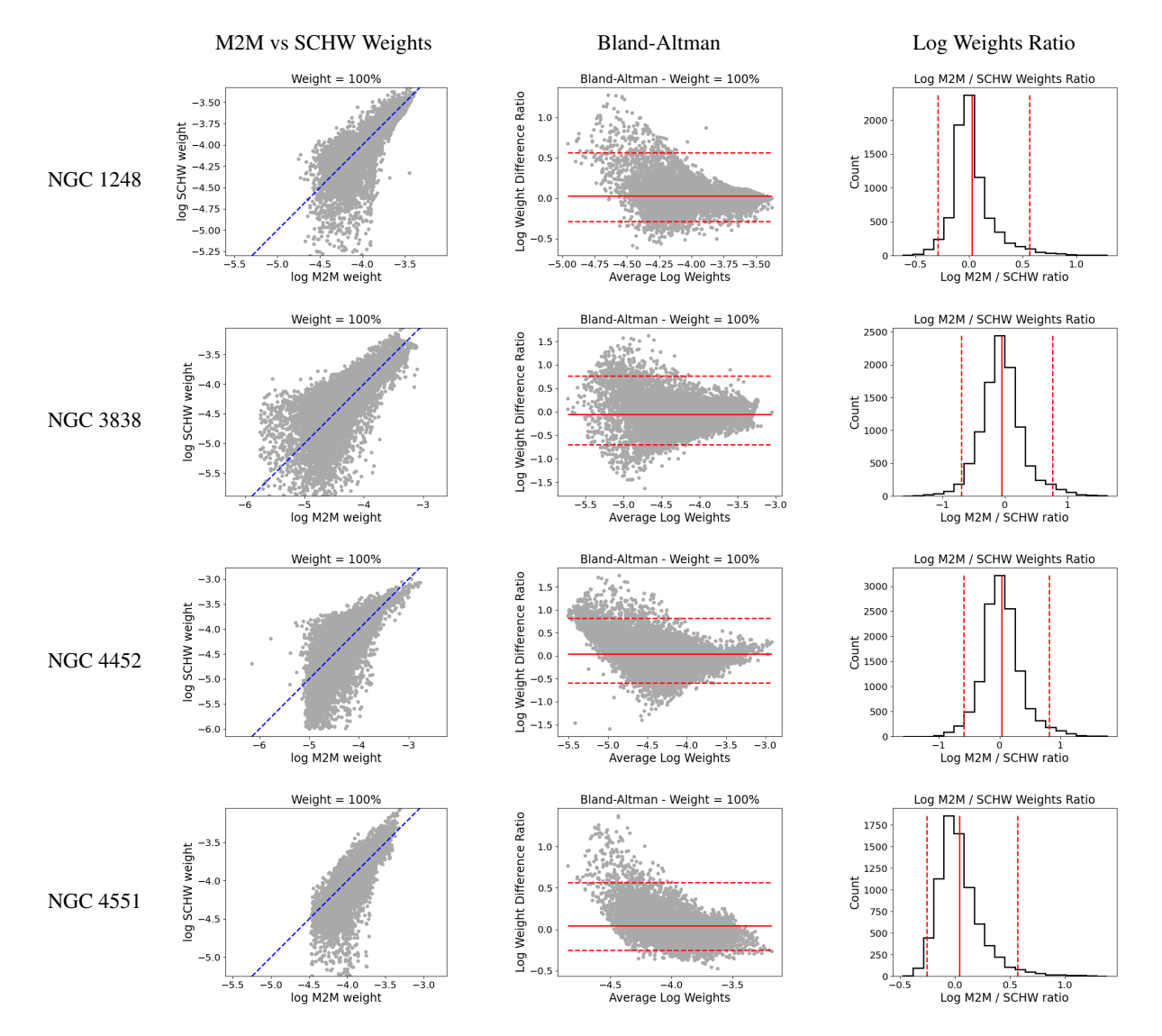


Fig. 2: M2M and SCHW Common Orbits Weight Comparison for ATLAS $^{\mathrm{3D}}$ Data

M2M and SCHW common orbits weight comparisons for ATLAS^{3D} data (Section 5.3). 3I initial conditions are used for the models. The left hand column shows scatter plots of the weights of the orbits, with the **blue** dashed line indicating equality of the orbit weights. The key point to note is that the weights are not tightly positioned close to the equality line: even though the orbits used are the same, M2M and SCHW are in general not allocating the same weights to the orbits. The Bland-Altman plots (Altman & Bland, 1983) of the average log weight for an orbit against the log difference between its M2M weight and its SCHW weight show that the mean log difference (**red** solid line) is approximately zero indicating that there is no significant bias towards either method. In addition, weight difference is larger at lower average weights than with larger average weights. The **red** dashed lines show the 2.5% and 97.5% percentiles with 95% of the difference ratios lying between the lines. The right hand plots show the distributions of the weight ratios. The **red** lines have the same meaning as in the Bland-Altman plots.

- 1. M2M and SCHW consistently achieve mean observable $\chi^2 \approx 1$ or less for both data sets and initial conditions. Related, M2M weight convergence is > 90%. In other words, both methods are able to reproduce observed data to an acknowledged, acceptable level (see Tables 4 and 5).
- 2. In terms of computer elapsed time, using the same computer configuration, M2M consistently outperforms SCHW. M2M elapsed times are between three and five times faster than SCHW (see Tables 4 and 5).

Table 8: 3I versus MDJV Comparisons for M2M and SCHW - Orbit Classifications

		3I Init	ial Condi	tions		1	MDJV I	nitial Con	ditions	
Galaxy	Active	(Orbit Clas	sificatio	n	Active	(Orbit Clas	sificatio	n
	Orbits	Hot	Warm	Cold	C-R	Orbits	Hot	Warm	Cold	C-R
Atlas3D – M2M										
NGC 1248	7977	0.18	0.41	0.23	0.17	8000	0.24	0.43	0.21	0.12
NGC 3838	14098	0.16	0.37	0.36	0.11	13742	0.27	0.51	0.16	0.06
NGC 4452	15896	0.17	0.31	0.34	0.17	15389	0.25	0.49	0.12	0.14
NGC 4551	7889	0.26	0.39	0.15	0.19	7882	0.39	0.46	0.03	0.13
Atlas3D - SCHW										
NGC 1248	7878	0.19	0.42	0.25	0.13	7804	0.25	0.45	0.17	0.13
NGC 3838	10484	0.22	0.39	0.31	0.07	12440	0.23	0.56	0.15	0.07
NGC 4452	13106	0.19	0.31	0.31	0.18	8678	0.19	0.51	0.13	0.17
NGC 4551	7771	0.30	0.38	0.13	0.18	7225	0.33	0.48	0.03	0.16
IllustrisTNG – M2M										
A0490	8000	0.36	0.28	0.13	0.23	8000	0.36	0.34	0.09	0.21
A1090	8000	0.30	0.43	0.15	0.12	8000	0.34	0.46	0.09	0.11
A1190	8000	0.39	0.40	0.08	0.13	8000	0.42	0.41	0.04	0.13
A1290	8000	0.31	0.34	0.20	0.14	7977	0.34	0.37	0.15	0.14
A1390	8000	0.33	0.42	0.12	0.13	8000	0.34	0.46	0.06	0.13
IllustrisTNG - SCHW										
A0490	4529	0.38	0.31	0.14	0.18	6084	0.37	0.34	0.09	0.20
A1090	5315	0.30	0.41	0.18	0.11	6906	0.35	0.46	0.10	0.10
A1190	5581	0.40	0.37	0.10	0.13	7379	0.43	0.40	0.04	0.13
A1290	5135	0.30	0.36	0.21	0.13	6984	0.34	0.38	0.15	0.13
A1390	5739	0.33	0.40	0.13	0.13	7219	0.35	0.46	0.06	0.12

The orbit classification comparisons for 3I and MDJV initial conditions (Section 5.4). Comparisons in the table are made horizontally with classification differences of $\geq 3\%$ between 3I and MDJV being indicated in **red**. 3I and MDJV do not produce the same orbit classifications, though it is interesting that there is less disagreement on the counter-rotating orbit classification.

- 3. For both data sets, M2M and SCHW produce orbit classifications which are approximately the same for the same initial conditions (Table 6), but are not the same for different initial conditions (Table 8). The classifications are dependent on the initial conditions.
- 4. Both M2M and SCHW using IllustrisTNG data as in Xu et al. (2019) do not produce orbit classifications which match those in Xu et al. (2019) (see Table 9). It therefore appears that the gravitational potential, observed data sets and initial conditions used by the methods are not able to produce good 'orbit level' representations of the associated galaxies.
- 5. M2M and SCHW, using the same gravitational potentials and initial conditions, do not use exactly the same orbits in reproducing the same observed data. For orbits which are common, these orbits do not have the same weights (see Figure 2).
- 6. Changing the data layout of surface brightness from one polar system to another does not appear to affect model results. However, changing the kinematical data layout from IFU Voroni cells to a polar system does cause the orbit classification results to change (see Table 11).

3I Initial Conditions Xu et al. (2019) **MDJV** Initial Conditions Galaxy Orbit Classification Orbit Classification Orbit Classification Hot Warm Cold C-R Hot Warm Cold C-R Hot Warm Cold C-R IllustrisTNG - M2M A0490 0.36 0.28 0.23 0.35 0.28 0.36 0.34 0.09 0.21 0.13 0.14 0.23 A1090 0.30 0.12 0.43 0.15 0.28 0.46 0.150.10 0.34 0.46 0.09 0.11 A1190 0.39 0.40 0.08 0.13 0.33 0.43 0.11 0.12 0.42 0.41 0.04 0.13 A1290 0.31 0.34 0.20 0.14 0.34 0.37 0.15 0.14 0.32 0.37 0.18 0.13 A1390 0.42 0.12 0.13 0.29 0.33 0.45 0.15 0.12 0.34 0.46 0.06 0.13 IllustrisTNG - SCHW A0490 0.38 0.31 0.14 0.18 0.35 0.37 0.34 0.09 0.20 0.28 0.14 0.23 A1090 0.30 0.41 0.18 0.11 0.28 0.15 0.10 0.35 0.46 0.10 0.10 0.46 A1190 0.40 0.37 0.10 0.13 0.33 0.43 0.11 0.12 0.43 0.40 0.04 0.13A1290 0.30 0.36 0.21 0.13 0.32 0.34 0.37 0.18 0.13 0.38 0.15 0.13

0.29

0.45

0.15

0.12

0.35

0.46

0.06

0.12

Table 9: IllustrisTNG M2M and SCHW Comparisons with Xu et al. (2019) - Orbit Classifications

Orbit classification comparisons for M2M and SCHW with Xu et al. (2019) (see Section 5.5). Comparisons in the table are made horizontally between models and Xu et al. (2019). Classification differences of $\geq 3\%$ with Xu et al. (2019) are indicated in **red** and **blue**. Apart from the A0490 M2M model, all the other models have some differences with Xu et al. (2019). The values in the counter-rotating columns are notable for their lack of differences. The MDJV cold column reflects differences between the initial conditions where MDJV has fewer cold orbits than 3I.

0.13

0.13

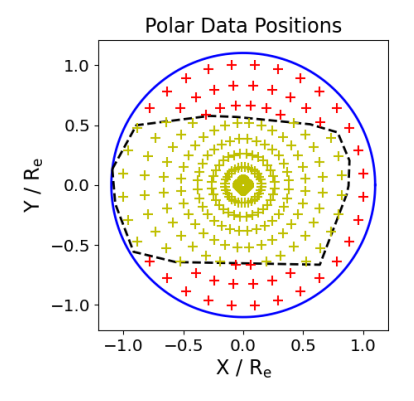
1.0 -0.5 0.0 0.5 1.0 X / Re

0.33

0.40

A1390

Fig. 3: Data Positions for NGC 4452



IFU and polar data positions for NGC 4452 kinematical data (Section 5.6). The left hand plot shows the IFU data positions in yellow with the black dashed line showing the convex hull enclosing the data points. The blue circle has the minimum radius necessary to surround all data points. This radius gives the extent of the polar grid in the right hand plot. In this plot, the yellow data points have data values interpolated from the IFU data values. The red points are the points in the polar grid that are outside of the convex and have no data values.

Nothing has come out of the investigation which indicates that the performance benefit that comes from using M2M should not be taken advantage of. The benefits to galaxy survey modeling are obvious. In addition, M2M is not affected by the performance limitations of using NNLS. Also, if the performance cost of NNLS were to be reduced to close to zero, M2M would still be faster. All that is required is for researchers to continue to be comfortable with modeling schemes using low orbit numbers to reproduce galaxy data, and with creating models that do not necessarily truly represent the parent galaxy and may actually be

Table 10:	Voronoi and	Polar	Kinematical	Data -	χ^2	Values
-----------	-------------	-------	-------------	--------	----------	--------

			Mean χ^2 values		M2M Weight
Galaxy	Orbits	sb	los v1	los v2	Convergence
Polar kinematical data					
NGC 1248	8000	0.38	0.23	0.25	99%
NGC 3838	16000	1.01	0.51	0.50	92%
NGC 4452	16000	1.16	0.31	1.07	96%
NGC 4551	8000	0.87	0.24	1.17	98%
Voronoi kinematical data					
NGC 1248	8000	0.31	0.27	0.63	99%
NGC 3838	16000	1.07	0.18	0.57	96%
NGC 4452	16000	0.76	0.42	0.69	96%
NGC 4551	8000	0.41	0.19	0.76	100%

The observable mean χ^2 values from the M2M ATLAS^{3D} polar versus Voronoi cells comparison (Section 5.6). All the χ^2 values are ≈ 1 or less, and the weight convergence values are > 90% indicting that M2M has reproduced the observed data as expected.

Table 11: Voronoi and Polar Kinematics - Orbit Classification

		Active	Orbit Classification			
Galaxy	Orbits	Orbits	Hot	Warm	Cold	C-R
Polar kinematics						
NGC 1248	8000	7782	0.21	0.41	0.23	0.15
NGC 3838	16000	12749	0.23	0.40	0.27	0.11
NGC 4452	16000	16000	0.18	0.28	0.28	0.25
NGC 4551	8000	7824	0.29	0.41	0.12	0.18
Voronoi kinematics						
NGC 1248	8000	7977	0.18	0.41	0.23	0.17
NGC 3838	16000	14098	0.16	0.37	0.36	0.11
NGC 4452	16000	15896	0.17	0.31	0.34	0.17
NGC 4551	8000	7889	0.26	0.39	0.15	0.19

The orbit classification values from the M2M ATLAS $^{\rm 3D}$ polar versus Voronoi cells comparison (Section 5.6). Table values in **red** indicate a classification difference of $\geq 3\%$. In total, there are nine **red** values suggesting that orbit classifications are dependent on the geometric arrangement of the observed data. The largest difference in classification is 9%.

non-physical (as another well-known scheme may do). Do not forget that, regardless of regularization, orbit selection within the methods is purely numerical and not astrophysical.

All comparisons between M2M and SCHW will, at some level, be implementation specific, but there seems to be little to be gained by seeking to address known modeling shortfalls in an SCHW-like context. M2M is inherently more flexible and scalable than SCHW. Orbit weights are available within the model from the outset so more complex observables are easier to model or estimate. Data uncertainties are an integral part of the M2M weight determination process, and are accommodated far more so than SCHW does in reaching the final solution. Once designed, achieving a basic M2M implementation in approximately six to eight weeks can be accomplished by an experienced programmer using a high level language such as Python, and including use of parallelization. Creating a GPU based implementation for M2M can be

achieved using tooling such as PyTorch (Paszke et al., 2019). However to gain the full performance benefits, this will require careful assessment and design of the GPU parallelizable features of M2M. Given that M2M employs a number of techniques that are used in machine learning, perhaps they might provide an alternative way forward and this will be investigated in the future by the authors

7 CONCLUSIONS

The objective set out in the Introduction to assess and compare the operational capabilities of M2M and SCHW has been met. Both methods are able to replicate observed data to an acceptable level but M2M outperforms SCHW being several times faster. This speed improvement makes M2M more desirable in a galaxy survey context than SCHW. Both methods produce similar orbit classifications for a given set of initial conditions, but the classifications do appear to be particular to the initial conditions used. In addition, the weights of the common orbits under-pinning the classifications differ and are method specific. Looking ahead, M2M is the more attractive option currently for stellar dynamical modeling in the 21st century, but could eventually be overtaken by machine learning based methods. However, in the mean time, this paper acts as a flag to the stellar dynamical modeling community that M2M should be seriously considered as a way of alleviating some of the shortcomings of SCHW.

Acknowledgements The author thanks Dandan Xu, Ling Zhu, Shude Mao and Yunpeng Jin for various fruitful discussions as the research recorded here progressed.

References

Altman, D. G., & Bland, J. M. 1983, Journal of the Royal Statistical Society. Series D (The Statistician), 32, 307

Behnel, S., Bradshaw, R., Citro, C., et al. 2011, Computing in Science Engineering, 13, 31

Cappellari, M. 2002, MNRAS, 333, 400

Cappellari, M., Emsellem, E., Krajnović, D., et al. 2011, MNRAS, 413, 813

Cappellari, M., Scott, N., Alatalo, K., et al. 2013, MNRAS, 432, 1709

Emsellem, E., Monnet, G., & Bacon, R. 1994, A&A, 285, 723

Lawson, C., & Hanson, R. 1974, Solving Least-Squares Problems (Prentice-Hall, New Jersey)

Lipka, M., & Thomas, J. 2021, MNRAS, 504, 4599

Long, R. J. 2016, Research in Astronomy and Astrophysics, 16, 189

Long, R. J. 2025, Research in Astronomy and Astrophysics, 25, 035011

Long, R. J., Lu, S.-D., & Xu, D.-D. 2021, Research in Astronomy and Astrophysics, 21, 152

Long, R. J., & Mao, S. 2010, MNRAS, 405, 301

Long, R. J., & Mao, S. 2012, MNRAS, 421, 2580

Nelson, D., Springel, V., Pillepich, A., et al. 2019, Computational Astrophysics and Cosmology, 6, 2

Paszke, A., Gross, S., Massa, F., et al. 2019, PyTorch: An Imperative Style, High-Performance Deep Learning Library, arXiv:1912.01703

Schwarzschild, M. 1979, ApJ, 232, 236

Syer, D., & Tremaine, S. 1996, MNRAS, 282, 223

Thomas, J., & Lipka, M. 2022, MNRAS, 514, 6203

Virtanen, P., Gommers, R., Oliphant, T. E., et al. 2020, Nature Methods, 17, 261

Xu, D., Zhu, L., Grand, R., et al. 2019, MNRAS, 489, 842

Zhu, L., van de Ven, G., van den Bosch, R., et al. 2018, Nature Astronomy, 2, 233

Appendix A: EXAMPLE OBSERVABLE REPRODUCTION

This appendix contains a visual example in Figure A.1 of the reproduction of observables by M2M and SCHW using NGC 4452 with 3I initial conditions (see Section 5.2).

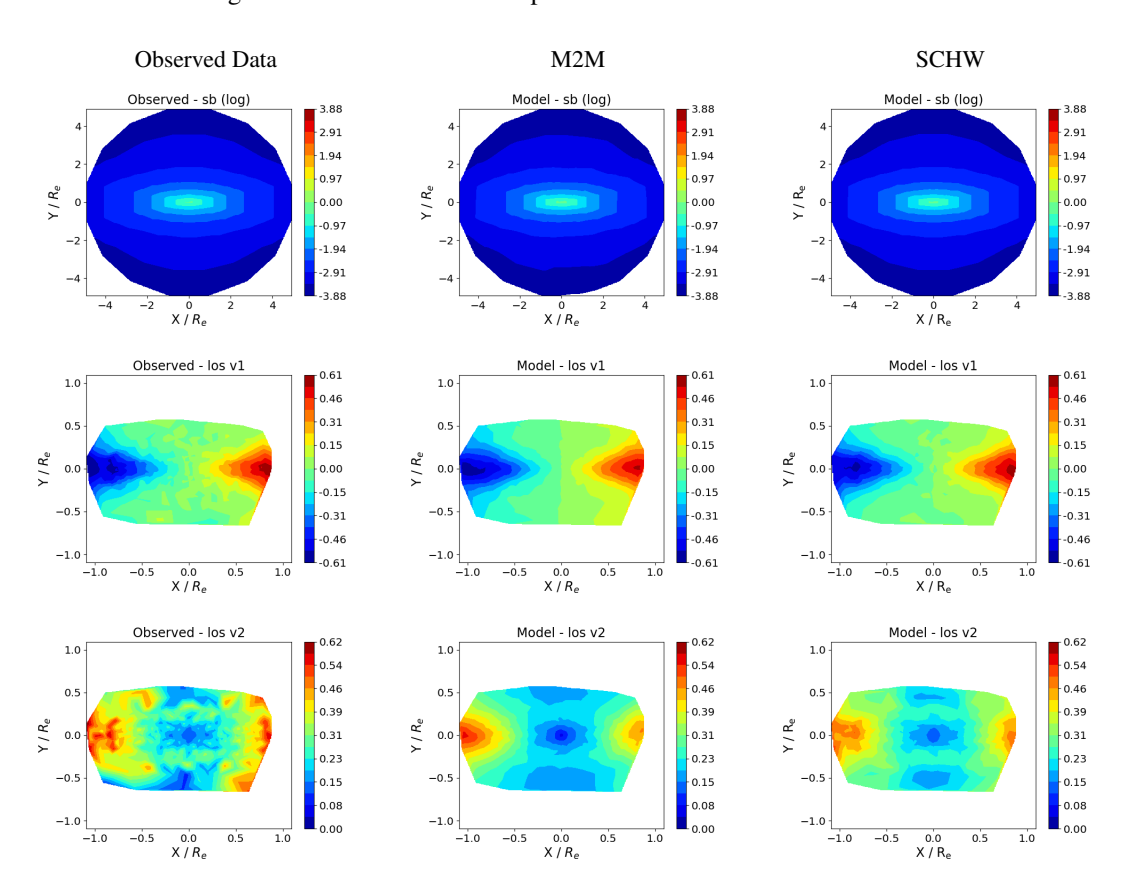


Fig. A.1: M2M and SCHW Reproduction of Observables - NGC 4452

Reproduction of observables by M2M and SCHW using NGC 4452 with 3I initial conditions (Appendix A). The observables are surface brightness in the top row followed by the first and second velocity moments. Units are as in Section 3. The first column displays the observed data used in modeling, with the second and third columns showing reproduction of the observed data by the modeling methods. In row order, the mean observable χ^2 values are (0.76, 0.42, 0.69) for M2M and (0.30, 0.13, 0.25) for SCHW (see Table 4).